

Performance Evaluation of a Semi-Transparent Photovoltaic Vacuum Glazing Panels

Ali Radwan¹, Takao Katsura¹, Saim Memon², Ahmed A. Serageldin¹, Makoto Nakamura¹, Katsunori Nagano¹

¹Division of Human Environmental Systems, Faculty of Engineering, Hokkaido University, Japan.

²School of Engineering, London South Bank University, 103 Borough Road, London, SE1 0AA, UK.

Abstract: A semi-transparent (50.8% transparency) CdTe solar cell strings-based glazing is integrated with structured-core translucent vacuum insulation panel and indium sealed vacuum glazing to modernize smart windows. Experimental analysis of semi-transparent photovoltaic glazing (GPV), vacuum glazing (VG), translucent vacuum insulation panel (GVIP), semi-transparent PV with VG (VGPV), semi-transparent PV with translucent vacuum insulation panel (VIPPV) were compared with single glazing (SG). The results show that VGPV achieved U-value compared to VIPPV. The steady-state measured center-of-pane temperature difference is around 55 °C, 32.5 °C and 5 °C for the VGPV, VIPPV, and GPV respectively under the solar irradiation of 1000 Wm⁻². The computationally estimated center-of-pane U-value of the VG, VGPV, VIPPV, GPV, and SG each dimensions of 15 cm × 15 cm, are predicted to be 1.3, 1.2, 1.8, 6.1 and 6.3 Wm⁻²K⁻¹ respectively.

1. Introduction

The increase in high-rise buildings construction with larger transparent facade demands the integration of progressive novel technologies in smart window sector [1]. Therefore, building Integrated Photovoltaic (BIPV) technologies become one of the most promising options to accomplish the needs for these sectors, where energy generation is advantageous [2]. In BIPV, the photovoltaic (PV) arrays were integrated on the exterior facades of the buildings. The PV system generates electricity for building needs and decreases the solar heat gain emerging the building or striking the outside surfaces. The thermal insulation for the exterior transparent facades plays an important role in reducing the thermal heat loss and energy requirements specifically for larger window-to-wall ratios in high-rise buildings. Therefore, using hybrid semi-transparent PV with higher thermal insulation efficiency is effective way to accomplish the both power generation and thermal insulation without compromising the facade area.

This study presents, an experimental performances of six different glazing systems that are: semi-transparent photovoltaic glazing (GPV), vacuum glazing (VG), translucent vacuum insulation panel (GVIP), semi-transparent PV with VG (VGPV), semi-transparent PV with translucent vacuum insulation panel (VIPPV) and for comparison single glazing (SG). These glazing systems are designed, constructed, and tested using the hot box calorimeter with and without indoor simulated solar radiation effect. During testing, the center-of-pane U-value, the transient

temperature variation of the inner, and outer surfaces of the glazing systems were compared. Further, the moisture condensation pattern is depicted for these systems.

3.1. Experimental setup

A transparent vacuum insulation panel (TVIP) is designed and developed. The current TVIP design uses a structured-core mesh with a transparent gas barrier envelope. This made it possible to resolve the complexity of the edge seal and subsequent construction cost issues that VG faces, mainly due to the edge seal such as indium. In addition, it also avoids the opaque characteristics of conventional VIPs. The core material is manufactured from a hollow polycarbonate frame encapsulated in a translucent multilayered polymeric envelope to keep the panel element semi-transparent. In addition, to decrease the inner radiation exchange, a L-e (low-emittance) film is used. This TVIP is attached to the SG, as the reference case for the retrofitting option. The frame dimensions are designed based on the structure model developed in [3]. The dimensions of the frame were $\delta = 1$ mm and $D = 8$ mm, with a total TVIP area of 150 mm × 150 mm. The compared glazing's are depicted in Fig.1.

Fig. 2 shows the experimental setup used for measuring the insulation performance of each glazing types. The experimental setup consists of temperature-controlled room and measuring devices. The temperature-controlled room has a door with area of 1.15 m × 0.6 m. This door is

fabricated from 5 cm thickness polystyrene foam insulation. In this door, a square area with dimensions of 15 cm×15 cm was cut. This square area is used to fix the proposed glazing. Six calibrated thermocouples were used to measure the temperatures at different locations in the apparatus as shown in Fig.2. Two thermocouples were used to measure the temperature across the glazing by measuring the inner and outer surfaces temperature of the glazing at the center of the glazing. Other two thermocouples were used to measure the temperatures at the inner and outer surfaces of the insulation wall. And the final two thermocouples were used to measure the inner and outer air temperatures inside and outside the calorimeter. Further, thermal infrared camera is used to measure the temperature contours on the outside glass pane of the samples. Furthermore, the laboratory relative humidity is measured using hygrometer.

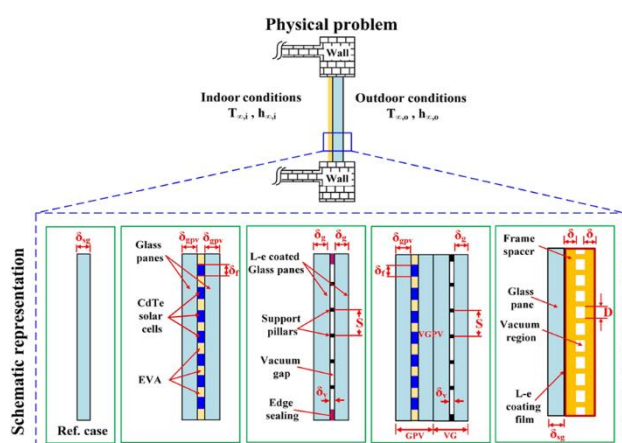


Fig. 1. Schematic diagram illustrating the real field application and schematic representation of the compared glazing types.

In this experiment, IR FLIR is used to measure the temperature contours on the front surfaces of the glazing's. The camera is focused to measure the temperature on a square area with dimensions larger than 20 cm × 20 cm. This area includes 15 cm × 15 cm for the sample and the rest is for the insulated calorimeter door. This allows us to compare the temperature contours of the sample compared to foam insulation door.

The samples were tested under two climatic conditions. The first without solar irradiation with calorimeter inner air temperature at -10 °C whilst the temperature outside the calorimeter at 25°C. The 25°C mimics the indoor temperature and the -10 °C mimics the outdoor weather conditions in a cold region such as in Sapporo, Hokkaido,

Japan (43.0618° N, 141.3545° E). To measure the electrical characteristics for the GPV sample alone and with the integration of VG and the TVIP insulations, another simulated climatic condition was used. In this testing condition, the air temperature inside the calorimeter was set to 25 °C mimicking the indoor thermal comfort. And the lab conditions were also kept at the same temperature of 25 °C whilst the solar irradiation is increased from 200 Wm⁻² to 1000 Wm⁻² using halogen lamps. The solar radiation is simulated using two identical halogen lamps. Each lamp has an aperture area of 25 cm × 15 cm. The halogen lamps were connected to a volt slider. This volt slider controls the light intensity. Semi-transparent GPV sample is tested as a base sample. Then this sample is integrated to VG and TVIP sample and tested under the same conditions. The temperatures at different locations on the glazing surfaces, insulation door, and air temperatures were measured. Further, the instantaneous open circuit voltage, steady state short-circuit current, steady state I-V characteristics and the steady state PV glazing power were measured at different solar irradiances.

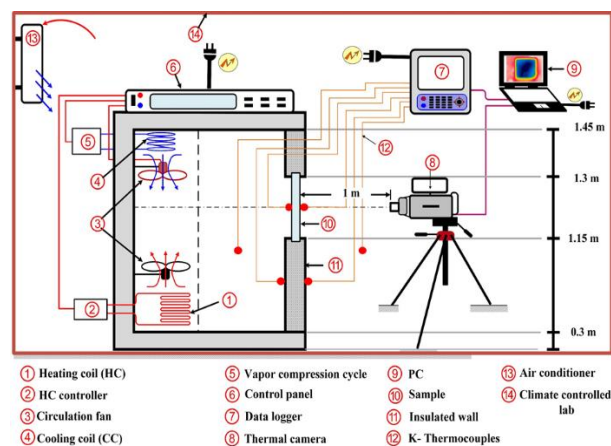


Fig. 2 Experimental setup for the thermal performance analysis of the glazing systems using hot-box calorimeter.

3.2. Results and discussion

Fig. 3 shows the instantaneous variation of $T_{\infty,in}$, $T_{\infty,o}$, $T_{g,in}$, $T_{g,o}$, $T_{ins,in}$ and $T_{ins,o}$ along with the moisture condensation pattern. All these temperatures started with a temperature of 25 °C and decrease with time. This decrease is caused by the operation of the calorimeter. In Fig. 3 (a), the variation of these temperatures for SG were displayed. The $T_{\infty,in}$ decreases with time until it reaches -10 °C and fluctuation starts because of the on/off control of the calorimeter. This fluctuation influences the

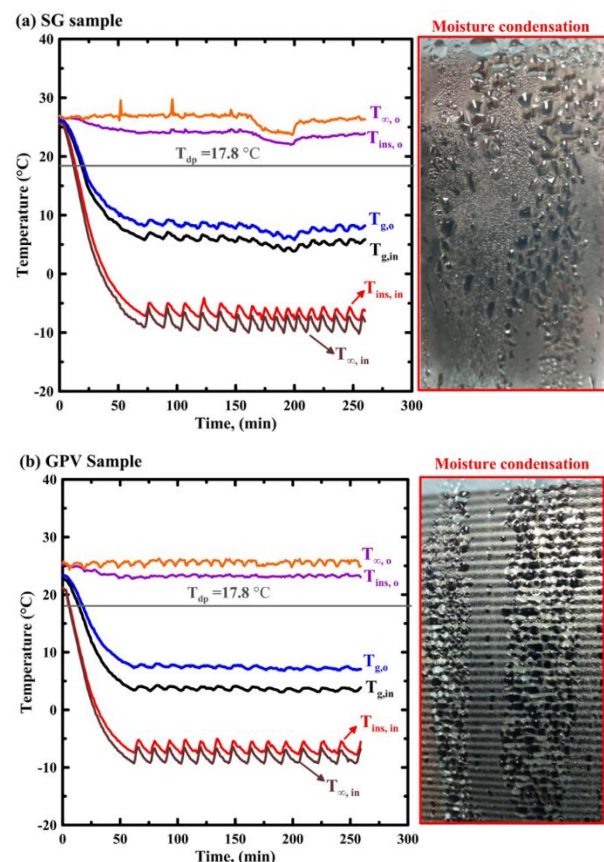
measured $T_{ins,in}$ taking the same trend. This temperature fluctuation influences the inner and outer glass temperatures $T_{g,in}$ and $T_{g,o}$. For the SG sample, the temperature difference across the SG sample at the steady state condition is only around 2.3 °C. It shows that for SG sample, with thermal conductivity of $0.85 \text{ Wm}^{-1}\text{K}^{-1}$ and thickness of 2.8 mm, the center heat flux is around 711 Wm^{-2} . In addition, the measured values for both $T_{g,in}$ and $T_{g,o}$ are lower than the dew point temperature of the air in the lab at $T_{\infty,o}$. This causes a higher moisture condensation over the outer surface of the pane. This moisture condensation decreases the vision level from the glazing. Although both $T_{g,in}$ and $T_{g,o}$ were smaller, no moisture condensation was observed on the surface with temperature of $T_{g,in}$. This is because of the inner air with temperature of $T_{\infty,in}$ decreases the dew point temperature of the air inside the calorimeter. Further, it is noticed that the temperature difference across the foam insulated wall is about 30.7 °C resulting to a smaller heat flux loss of 25.7 Wm^{-2} from $T_{\infty,in}$ to $T_{\infty,o}$ through the 5 cm thickness. Therefore, the heat flux through the SG represents around 27 times the heat loss than the foam wall.

In Fig. 3(b), the same temperatures were measured at the same testing conditions for the GPV sample. Similar trend was measured except a larger temperature difference across the glazing sample. This is because the total thermal conductivity of this sample is $0.3 \text{ Wm}^{-1}\text{K}^{-1}$ with total thickness of 6.3 mm. Such smaller value of thermal conductivity with larger thickness increases the glazing thermal resistance. Therefore, the heat flux transfer through this sample decreased to 172.8 Wm^{-2} . Whilst, it remains constant for the foam wall. Also, it is observed that the outer temperature of the GPV sample, $T_{g,o}$, still less than the laboratory dew point temperature. Therefore, the moisture condensation occurs as seen in the right-hand side of Fig. 3(b).

In Fig. 3(c), VG sample is tested. The temperature difference across the glazing become very high around 28.8 °C. This due to the significant decrease in the steady state heat flux transfer through the glazing to 37.6 Wm^{-2} which represents around 1.5 times than the heat transfer flux through the foam insulation wall. The measured $T_{g,o}$ is slightly affected by the temperature fluctuation inside the calorimeter. Furthermore, the outside surface temperature of the pane, $T_{g,o}$, increases above the dew point temperature

of the laboratory air. This prevents the moisture condensation problem on the surfaces of the glazing system.

To further enhance the insulation performance and allow electrical power generation from the glazing, the VGPV sample was tested Fig. 3 (d). The same trend for the VG sample is obtained with high temperature difference across the sample to reach 27 °C with glazing heat flux of 36 Wm^{-2} for a sample thickness of 13.3 mm. The moisture condensation is not appeared. Fig. 3(e) shows the measured temperature for the GVIP sample. In this sample, the TVIP was fabricated at the vacuum pressure of 0.25 Pa and attached to 2.8 mm glass layer. It is found that the temperature differences across the two sides of the window is around 19.7 °C. This results in a steady state heat flux of 79.3 Wm^{-2} , which represents around 3 times of heat flux through the foam wall. In addition, a slight condensation is observed on the surfaces of the glazing. In comparison, the moisture condensation starts after 20 min, 25min, and 45 min for SG, GPV, and VIPG glazing systems respectively. And visually, the largest condensation rate occurs in SG followed by GPV and then GVIP sample.



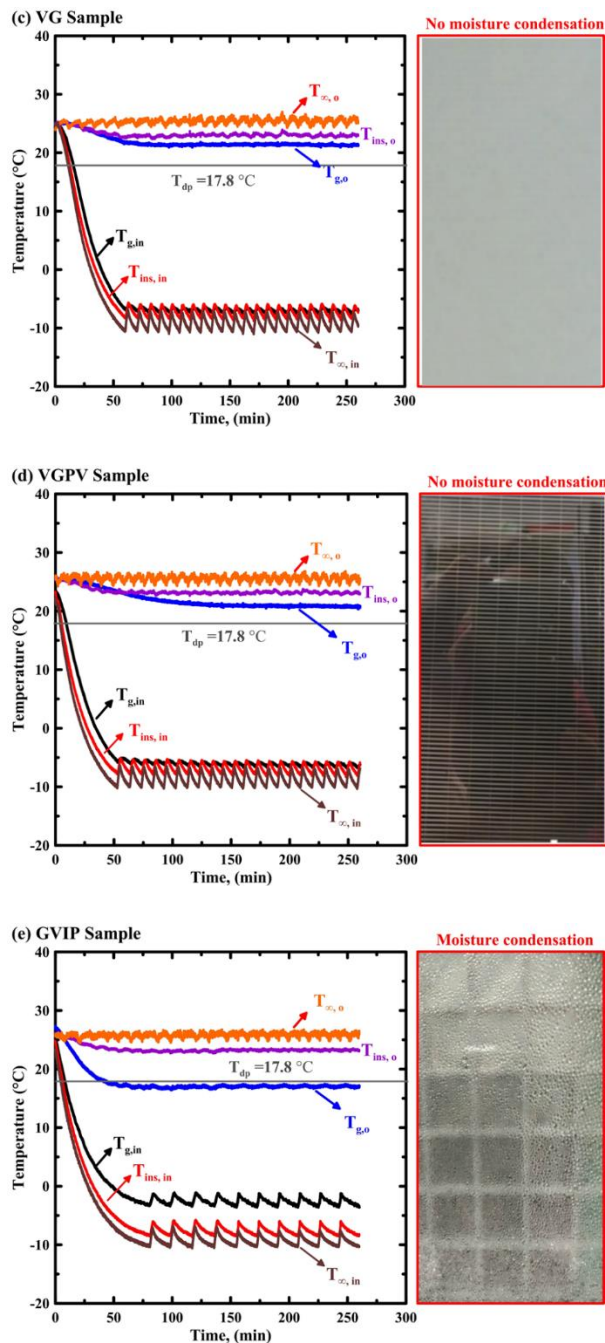


Fig. 3 Transient variation of the measured temperatures with condensation pattern for (a) SG sample, (b) GPV sample, (c) VG sample, (d) VGPV sample, and (e) GVIP glazing systems.

Fig. 4 display the variation of the glazing temperature difference and the open circuit voltage with the illumination time at the same solar radiation. The measured temperature differences increases with time and highest for VGPV sample as in Fig. 4-a. The measured V_{oc} decreases with the illumination time. This is because of the increase of solar cell temperature with the illumination time. The V_{oc} decreases from 9.75 V to 8.8 V for GPV sample, from

10 V to 8.3 V for VIPPV sample, and from 9.75 V to 7.7 V for VGPV sample after illumination time of 200 min. The maximum decrease in the V_{oc} is accomplished for VGPV sample because for high thermal insulation performance of the VG. The percent decrease in V_{oc} in VGPV glazing's in comparison with the conventional GPV sample represents around 12.5%. While the heat flux transfer through the VGPV sample decreased by 80 % compared with the GPV.

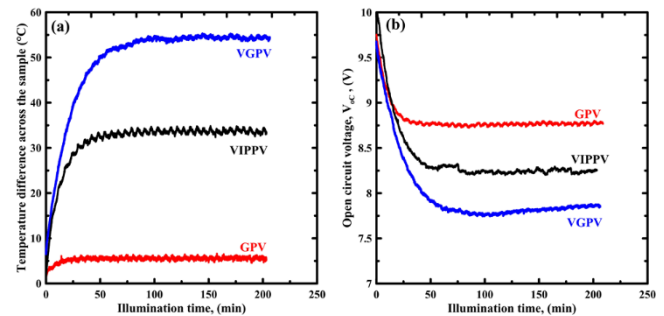


Fig. 4 Instantaneous comparison of (a) temperature difference across the samples and (b) measured open circuit voltages of the samples at solar radiation of 1000 W/m^2 .

Conclusions

1. The steady state measured center-of-pane temperature differences are $55 \text{ }^\circ\text{C}$, $32.5 \text{ }^\circ\text{C}$ and $5 \text{ }^\circ\text{C}$ for the VGPV, VIPPV, and GPV respectively at 1000 Wm^{-2} radiation.
2. At radiation of 1000 Wm^{-2} , the steady state open circuit voltage was 8.75, 8.25, and 7.85 V for GPV, VIPPV, and VGPV samples respectively.
3. The predicted center-of-pane U-value for VG, VGPV, VIPPV, and GPV samples, under ASTM boundary conditions were 1.3, 1.2, 1.8, and $6.1 \text{ Wm}^{-2}\text{K}^{-1}$ respectively

References

- [1] Y. Sun, R. Wilson, and Y. Wu, "A Review of Transparent Insulation Material (TIM) for building energy saving and daylight comfort," *Appl. Energy*, vol. 226, pp. 713–729, 2018.
- [2] L. Pan, R. Yan, H. Huang, H. He, and P. Li, "Experimental study on the flow boiling pressure drop characteristics in parallel multiple microchannels," *Int. J. Heat Mass Transf.*, vol. 116, pp. 642–654, 2018.
- [3] Z. Yang, T. Katsura, M. Aihara, M. Nakamura, and K. Nagano, "Investigation into window insulation retrofitting of existing buildings using thin and translucent frame-structure vacuum insulation panels," *Energies*, vol. 11, no. 2, 2018.